



# OPEN Dihydrotestosterone and 17 $\beta$ -estradiol modulate TMJ osteoarthritis development and reveal sex-specific differences in pathogenesis

Takuma Tomura<sup>1</sup>, Takenobu Ishii<sup>1</sup>✉, Norio Kasahara<sup>2</sup> & Yasushi Nishii<sup>1</sup>

To investigate the effects and mechanisms of dihydrotestosterone (DHT) and 17 $\beta$ -estradiol on temporomandibular joint osteoarthritis (TMJ-OA) to understand sex differences and apply findings to TMJ-OA prevention and treatment. Ten-week-old male C57BL/6J mice were divided into six groups to study the effects of mechanical stress (MS), aromatase inhibitors (Ai), orchiectomy (ORX), and 17 $\beta$ -estradiol supplementation on TMJ-OA. Interventions included mechanical stress induction and hormone manipulations. Analyses included serum hormone levels, micro-CT, histomorphometry, immunohistochemistry, RT-qPCR for gene expression, and statistical evaluations. ORX and Ai-induced reductions in DHT and 17 $\beta$ -estradiol caused bone loss, including decreased BV/TV and trabecular thickness, and increased trabecular spacing. MS further reduced cartilage thickness, Safranin O-positive areas, and increased osteoclast counts. Matrix metalloproteinase-13 (MMP13) and a disintegrin and metalloproteinase with thrombospondin motifs 5 (ADAMTS5) levels were highest in MS + Ai and MS + Ai + ORX groups. In contrast, 17 $\beta$ -estradiol supplementation restored cartilage thickness, reduced osteoclast activity, suppressed inflammatory markers (*NF $\kappa$ B*, *Gremlin 1*, *RelA*), and increased *BMP7* expression. The lower incidence of TMJ-OA in males may result from testosterone and DHT being converted to 17 $\beta$ -estradiol by adrenal aromatase, mitigating mechanical stress effects and protecting the temporomandibular joint via the *Gremlin-1-NF- $\kappa$ B* pathway.

**Keywords** Temporomandibular joint, Osteoarthritis, 17 $\beta$ -Estradiol, Dihydrotestosterone, Aromatase, Mechanical stress

Temporomandibular joint osteoarthritis (TMJ-OA) is a progressive disorder characterized by degenerative changes primarily affecting the articular cartilage, articular disc, synovium, mandibular condyle, and glenoid fossa. Pathological changes include cartilage destruction, granulation tissue formation, bone resorption, and apposition<sup>1–3</sup>. Clinically, TMJ-OA presents with symptoms such as joint sounds, jaw movement disorders, and pain around the temporomandibular joint. Non-reducible anterior disc displacement is commonly observed, often leading to perforation or rupture of the disc as the condition progresses. Advanced TMJ-OA results in deformation of the mandibular condyle, glenoid fossa, or articular eminence due to bone resorption and apposition, causing posterior and downward rotation of the mandible, anterior open bite, and skeletal maxillary protrusion<sup>4</sup>. While TMJ-OA affects both sexes, studies on males are limited due to its lower prevalence compared to females<sup>5</sup>.

Risk factors for TMJ-OA include excessive mechanical stress (MS), hormonal factors, aging, and systemic diseases. Excessive MS reduces cartilage layers, induces vascular endothelial growth factor (VEGF), and activates hypoxia-inducible factor-1 (HIF-1), leading to increased angiogenesis and osteoclast activity<sup>3–8</sup>. Hormonal abnormalities are another critical factor<sup>3</sup>. In females, gonadotropin-releasing hormone (GnRH) secreted from the hypothalamus stimulates the pituitary gland to release follicle-stimulating hormone (FSH) and luteinizing hormone (LH), which, in turn, stimulate the ovaries to produce estrogen and progesterone. Although this system

<sup>1</sup>Department of Orthodontics, Tokyo Dental College, 2-9-18 Kandamisaki-cho, Chiyoda-ku, Tokyo 101-0061, Japan.

<sup>2</sup>Department of Histology and Developmental Biology, Tokyo Dental College, 2-9-18 Kandamisaki-cho, Chiyoda-ku, Tokyo 101-0061, Japan. ✉email: ishiit@tdc.ac.jp

is typically regulated by feedback mechanisms, conditions such as menstrual irregularities or menopause reduce the production of  $17\beta$ -estradiol, increasing the risk of osteoporosis and potentially contributing to TMJ-OA<sup>3,9,10</sup>.

In males, sex hormones are primarily derived from cholesterol, converted into dehydroepiandrosterone (DHEA), and subsequently into testosterone. Testosterone is further metabolized into dihydrotestosterone (DHT) by 5- $\alpha$  reductase or into  $17\beta$ -estradiol by aromatase. Studies have shown that  $17\beta$ -estradiol protects against cartilage destruction in inflammatory-induced knee joints in male mice<sup>11,12</sup>. TMJ-OA is more prevalent in females than males, with a reported ratio of 3:1<sup>5</sup>. Hormonal stability differences may explain this disparity, as the incidence of hypogonadism in males aged 20–29 is approximately 5%, whereas menstrual irregularities are reported in 80.7% of females with an average age of 20.9 years<sup>4</sup>. Moreover, the age-related decline in DHT and  $17\beta$ -estradiol occurs more slowly in males than females, potentially influencing the lower TMJ-OA prevalence in males<sup>13</sup>. However, the detailed relationship between TMJ-OA and sex hormone metabolites remains unclear.

This study aims to elucidate the reasons behind the lower incidence of TMJ-OA in males compared to females and explore the effects and mechanisms of DHT and  $17\beta$ -estradiol on TMJ-OA to apply these findings to its prevention and treatment.

## Results

### Development of the TMJ-OA model and systemic effects of sex hormones

The experiment was initiated simultaneously for all groups. Orchiectomy (ORX) was performed in the ORX group to reduce DHT levels through gonadectomy<sup>14,15</sup>. After a 3-week recovery period post-ORX, aromatase inhibitors were administered intraperitoneally in the Ai group using an ALZET pump<sup>16</sup>. Four weeks after the experiment began, excessive mechanical stress (MS) was applied to the MS group by fixing a metal plate at a 45-degree incline on the maxillary incisors using composite resin to induce posterior displacement of the mandible during occlusion (Fig. 1a, b). The effects of ORX and aromatase inhibitors were assessed by evaluating serum hormone levels. Mice treated with aromatase inhibitors showed significantly reduced levels of  $17\beta$ -estradiol compared to untreated mice. In the ORX group, although no significant changes in testosterone

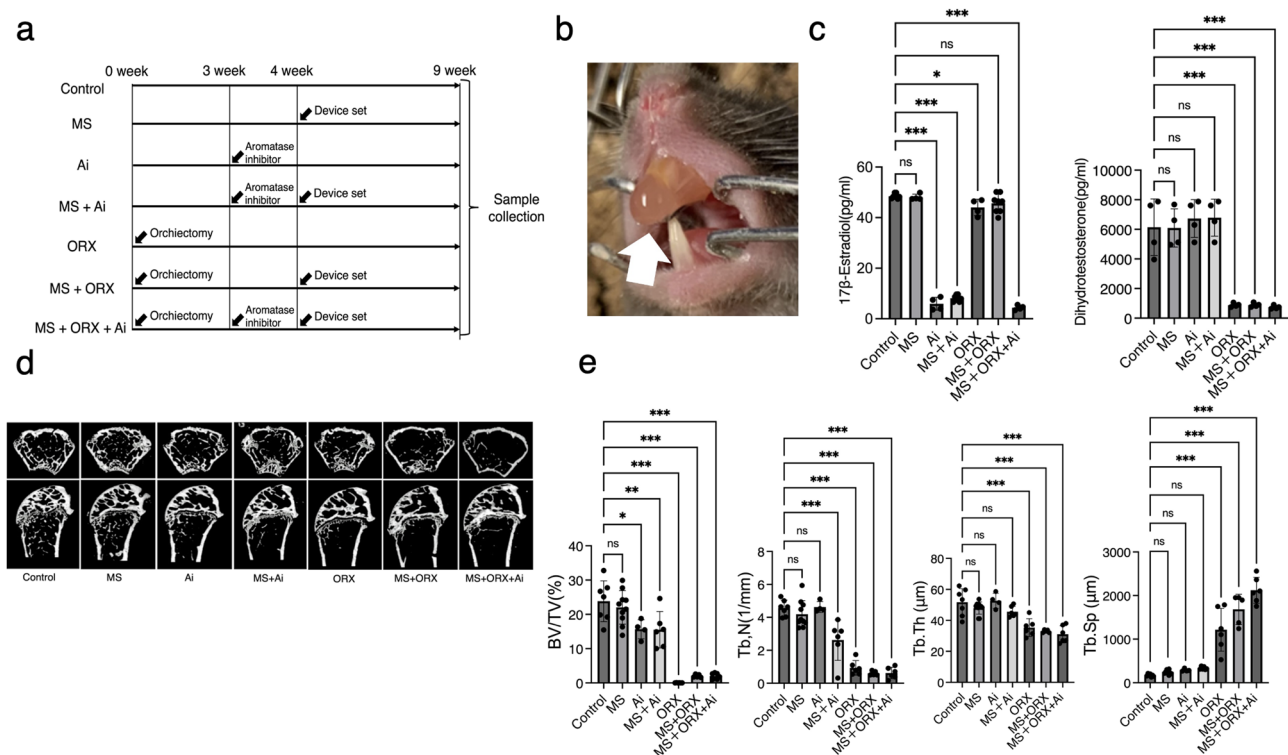


**Fig. 1.** Experimental design and systemic effects of hormone manipulation. (a) Experimental protocol: 10-week-old mice were divided into seven groups (control, MS, Ai, MS + Ai, ORX, MS + ORX and MS + Ai + ORX). Orchiectomy (ORX) was performed at the beginning of the experiment, and after a 3-week healing period, aromatase inhibitors (Ai) were implanted intraperitoneally in the ALZET pump for the ORX group. Four weeks after the start of the experiment, a metal plate was placed in the group subjected to mechanical stress (MS) on the TMJ. Nine weeks after the start of the experiment, the animals were slaughtered and the samples were collected. (b) Apparatus: A metal plate with a base thickness of 2 mm was attached to the posterior surface of the maxillary portal teeth with composite resin to induce an unbalanced occlusion. (c) Measurement of dihydrotestosterone and  $17\beta$ -estradiol levels in serum using ELISA. \* $P < 0.033$ , \*\* $P < 0.002$ , \*\*\* $P < 0.001$ , ns = no significance. (d)(e) The results of femoral bone structure analysis in the seven groups are shown. Tb.Th (trabecular thickness), Tb.N (number of trabeculae), Tb.S (trabecular separation), and Tb.Sp (trabecular spacing) were measured. \*\*\* $P < 0.001$ , ns = no significance.

levels were observed,  $17\beta$ -estradiol levels significantly decreased along with a reduction in testosterone levels compared to untreated mice. The amount of  $17\beta$ -estradiol was significantly lower in the Ai group compared to the ORX group, while testosterone levels significantly decreased in the ORX group (Fig. 1c). Bone structure analysis of the femur revealed that groups treated with aromatase inhibitors and ORX exhibited reduced BV/TV (%), trabecular number (1/mm), and trabecular thickness ( $\mu\text{m}$ ), along with increased trabecular spacing ( $\mu\text{m}$ ) compared to the control group (Fig. 1d, e).

### TMJ-OA induced by DHT reduction and excessive mechanical stress

Paraffin sections of the mandibular condyles from mice were stained with H&E to evaluate cartilage thickness. Groups subjected to mechanical stress (MS group and MS + ORX group) showed a significant reduction in cartilage thickness compared to the control group. Safranin O staining revealed a significant decrease in Safranin O-positive areas and a significant increase in modified Mankin scores in the MS and MS + ORX groups (Fig. 2a, b). TRAP staining was performed to quantify the number of osteoclasts in the mineralized bone layer beneath the cartilage. The osteoclast counts significantly increased in all experimental groups compared to the control group, with the MS + ORX group showing approximately a threefold increase in osteoclast numbers compared to the control group. Additionally, Safranin O staining confirmed a significant reduction in Safranin O-positive areas and an increase in modified Mankin scores in the MS and MS + ORX groups (Fig. 2a, b). Furthermore, strong expression of Matrix metalloproteinase-13 (MMP13) and A disintegrin and metalloproteinase with thrombospondin motifs 5 (ADAMTS5) was observed in the mineralized bone layer beneath the cartilage in both the MS and MS + ORX groups (Fig. 2c). In the semi-quantitative analysis of MMP13 and ADAMTS5 expression, the ORX group showed a significant increase compared to the control group. Furthermore, the MS group exhibited significantly higher expression levels than the ORX group. Notably, the combination of mechanical stress and orchietomy further enhanced the expression, with the MS + ORX group showing significantly higher levels of MMP13 and ADAMTS5 compared to the MS group (Fig. 2d).

### TMJ-OA induced by $17\beta$ -estradiol reduction and excessive mechanical stress

Paraffin sections of the mandibular condyles from mice were stained with H&E to evaluate cartilage thickness. Groups exposed to excessive mechanical stress (MS group and MS + Ai group) showed a significant reduction in cartilage thickness compared to the control group. Safranin O staining revealed a significant decrease in Safranin

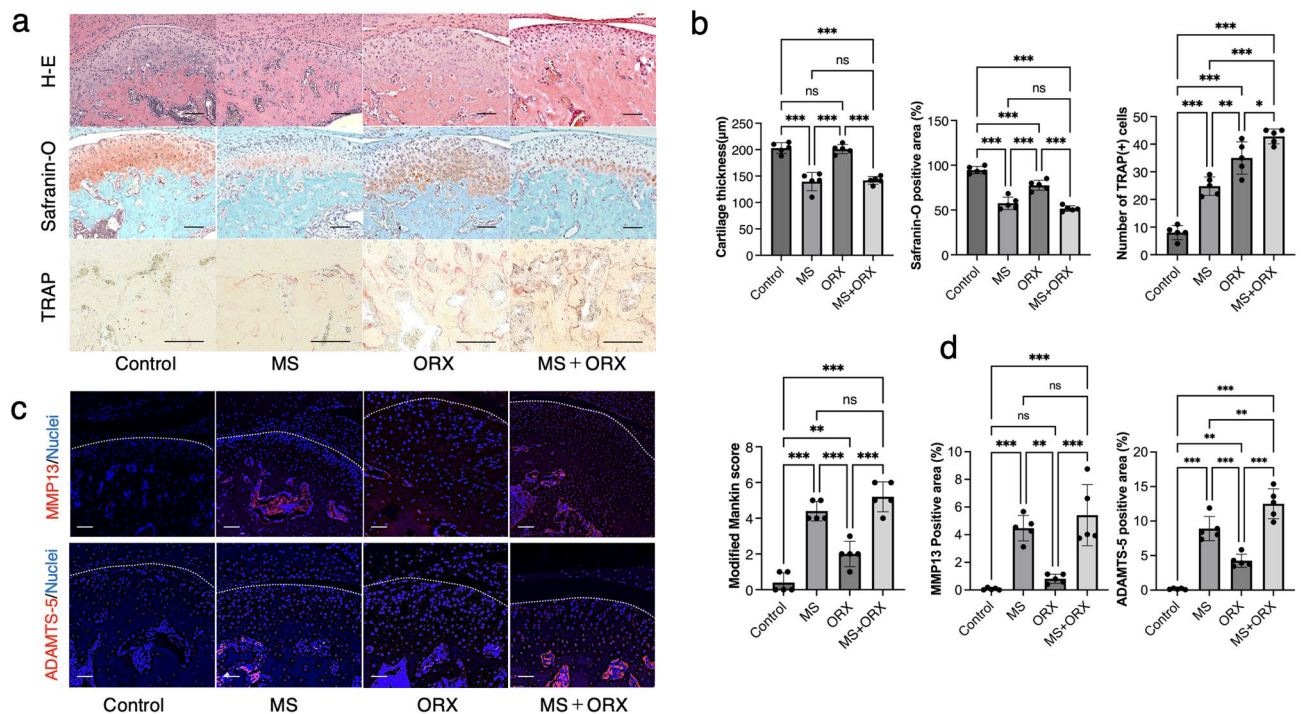


**Fig. 2.** Effects of DHT reduction and mechanical stress on TMJ cartilage. (a) Histochemical staining of the mandibular head of a male mouse is shown. Cartilage thickness was confirmed by H-E staining (scale bar = 100  $\mu\text{m}$ ). Positive areas were measured by safranin-O staining (scale bar = 100  $\mu\text{m}$ ). The number of osteoclasts per  $\text{mm}^2$  was measured by TRAP staining (scale bar = 100  $\mu\text{m}$ ). (b) Cartilage thickness measured on H-E stained sections. Proteoglycan area in Safranin-O stained sections. mean number of osteoclasts per  $\text{mm}^2$  ( $N > 3$  nuclei) in TRAP stained sections. Results of the Modified Mankin score for OA severity assessment. (c) Immunohistochemical staining of the mouse mandibular head for MMP13 (scale bar = 100  $\mu\text{m}$ ; MMP13: red, nuclei: blue) and ADAMTS5 (scale bar = 100  $\mu\text{m}$ ; ADAMTS5: red, nuclei: blue). (d) Semi-quantitative analysis of MMP13 and ADAMTS5 expression comparing the control, MS, ORX, and MS + ORX groups. \* $P < 0.033$ , \*\* $P < 0.002$ , \*\*\* $P < 0.001$ , ns = no significance.



O positive areas and an increase in modified Mankin scores in the MS and MS + Ai groups. TRAP staining was performed to quantify the number of osteoclasts in the mineralized bone layer beneath the cartilage. Osteoclast counts were significantly higher in all experimental groups compared to the control group, with the MS + Ai group showing approximately a threefold increase in osteoclast numbers compared to the control group (Fig. 3a, b). In addition, MMP13 and ADAMTS5, key enzymes involved in cartilage destruction in TMJ osteoarthritis, were strongly expressed in the mineralized bone layer beneath the cartilage in both MS and MS + Ai groups. In the MS + Ai group, strong expression of these enzymes was also observed in the cartilage layer (Fig. 3c). In the semi-quantitative analysis of MMP13 and ADAMTS5 expression, no significant difference was observed between the control and Ai groups. However, the expression levels were significantly elevated when mechanical stress was applied. Notably, the combination of mechanical stress and aromatase inhibitor treatment resulted in a marked increase in the expression of both enzymes (Fig. 3d).

### TMJ-OA induced by reduction of 17 $\beta$ -estradiol and DHT combined with excessive mechanical stress

Paraffin sections of the mandibular condyles from mice were stained with H&E to evaluate cartilage thickness. In the MS + Ai + ORX group, cartilage thickness was significantly reduced compared to all other groups, and the MS + Ai group also showed a significant reduction compared to the MS + ORX group. Safranin O staining revealed significant decreases in Safranin O-positive areas and increases in modified Mankin scores in the MS + Ai, MS + ORX, and MS + Ai + ORX groups. To quantify osteoclast numbers in the mineralized bone layer beneath the cartilage, TRAP staining was performed, and the number of osteoclasts per square millimeter was counted. All experimental groups showed significant increases in osteoclast numbers compared to the control group, with the MS + Ai + ORX group exhibiting a fourfold increase compared to the control group. Additionally, the MS + ORX group showed significantly fewer osteoclasts compared to the MS + Ai group (Fig. 4a, b). In the group subjected to mechanical stress (MS), strong expression of MMP13 and ADAMTS5 was observed in both the mineralized layer of the subchondral bone and the chondrocyte layer. Furthermore, in the group treated with both aromatase inhibitors and orchietomy (MS + Ai + ORX), expression of MMP13 and ADAMTS5 extended to the superficial layer of the cartilage (Fig. 4c). In the semi-quantitative analysis of MMP13 and ADAMTS5

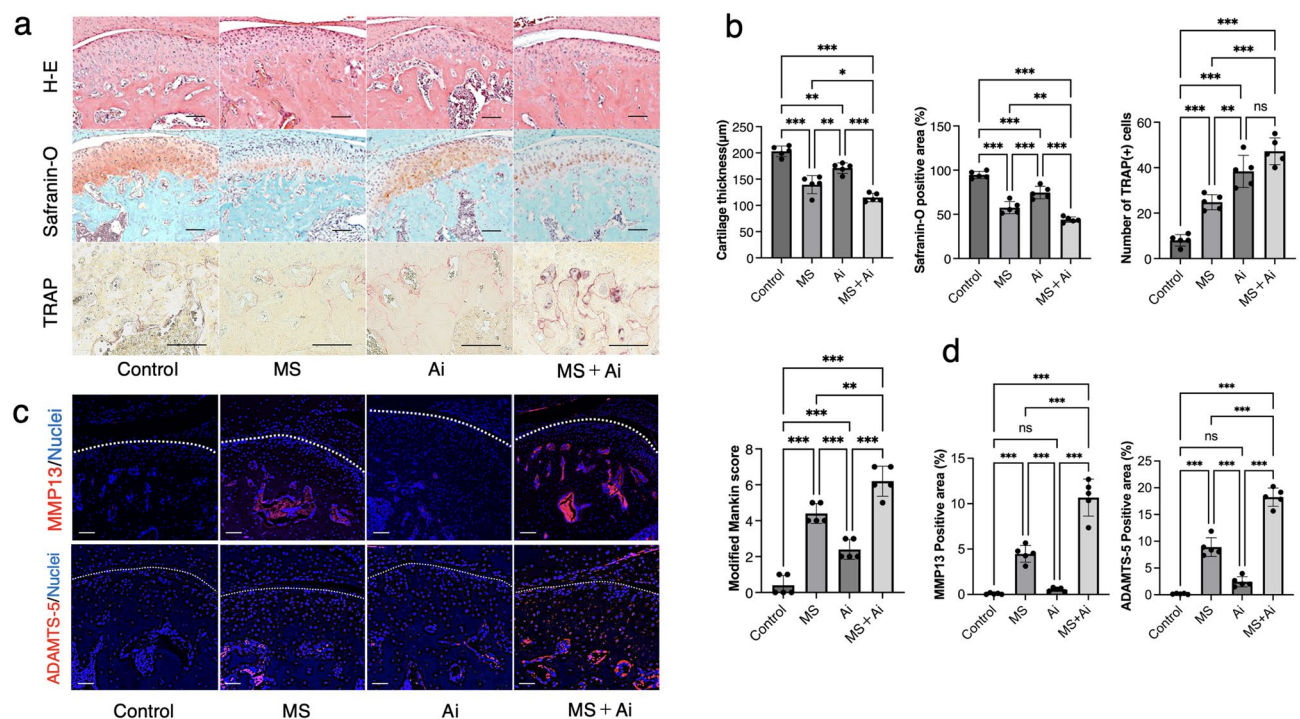


**Fig. 3.** Impact of 17 $\beta$ -estradiol deficiency on TMJ degeneration under mechanical stress. (a) Histochemical staining of the mandibular head of a male mouse is shown. Cartilage thickness was confirmed by H-E staining (scale bar = 100  $\mu$ m). Positive areas were measured by safranin-O staining (scale bar = 100  $\mu$ m). The number of osteoclasts per mm<sup>2</sup> was measured by TRAP staining (scale bar = 100  $\mu$ m). (b) Cartilage thickness measured on H-E stained sections. Proteoglycan area in Safranin-O stained sections. mean number of osteoclasts per mm<sup>2</sup> ( $N > 3$  nuclei) in TRAP stained sections. Results of the Modified Mankin score for OA severity assessment. \*\* $P < 0.002$ , \*\*\* $P < 0.001$ , ns = no significance. (c) Immunohistochemical staining of the mouse mandibular head for MMP13 (scale bar = 100  $\mu$ m; MMP13: red, nuclei: blue) and ADAMTS5 (scale bar = 100  $\mu$ m; ADAMTS5: red, nuclei: blue). ADAMTS5 were clearly expressed in the subchondral bone in MS and MS + ORX group. (d) Semi-quantitative analysis of MMP13 and ADAMTS5 expression comparing the control, MS, Ai, and MS + Ai groups. \* $P < 0.033$ , \*\* $P < 0.002$ , \*\*\* $P < 0.001$ , ns = no significance.

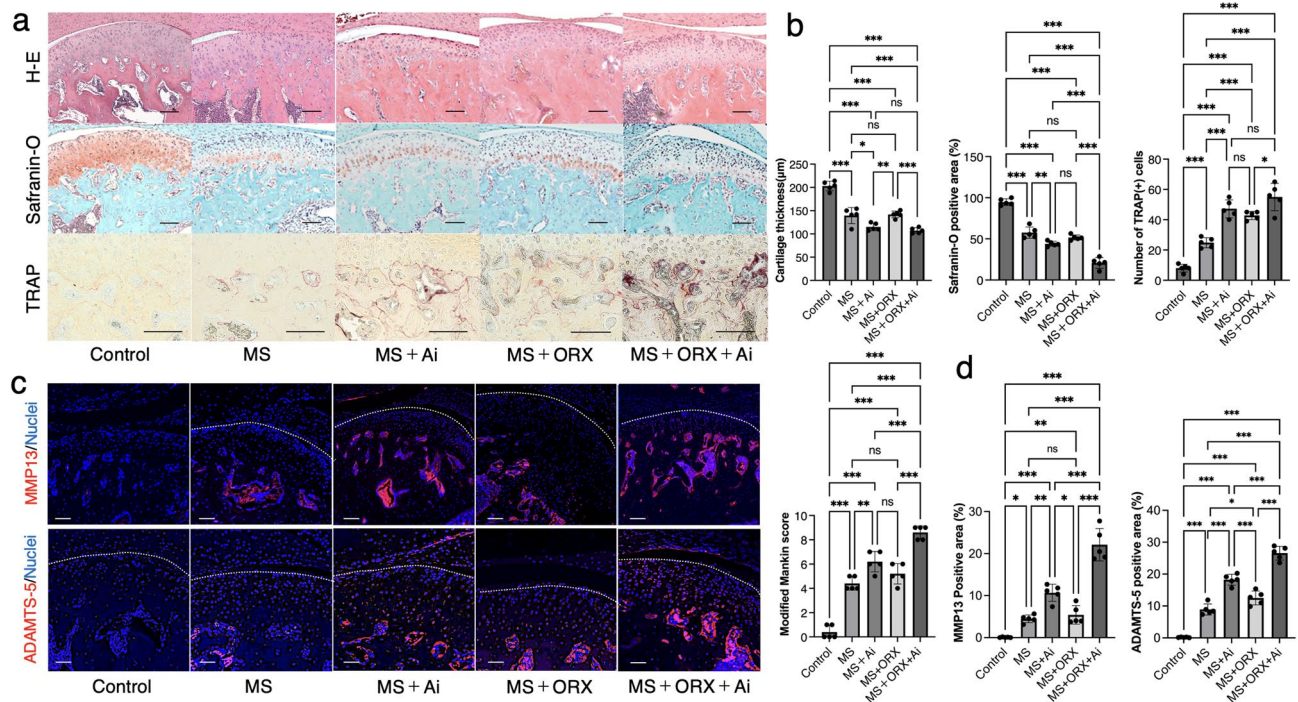


**Fig. 4.** Combined effects of DHT and 17β-estradiol deficiency with mechanical stress. (a) Histochemical staining of the mandibular head of a male mouse is shown. Cartilage thickness was confirmed by H-E staining (scale bar = 100 μm). Positive areas were measured by safranin-O staining (scale bar = 100 μm). The number of osteoclasts per mm<sup>2</sup> was measured by TRAP staining (scale bar = 100 μm). (b) Cartilage thickness measured on H-E stained sections. Proteoglycan area in Safranin-O stained sections. mean number of osteoclasts per mm<sup>2</sup> ( $N > 3$  nuclei) in TRAP stained sections. Results of the Modified Mankin score for OA severity assessment. \* $P < 0.033$ , \*\* $P < 0.002$ , \*\*\* $P < 0.001$ , ns = no significance. (c) Immunohistochemical staining of the mouse mandibular head for MMP13 (scale bar = 100 μm; MMP13: red, nuclei: blue) and ADAMTS5 (scale bar = 100 μm; ADAMTS5: red, nuclei: blue). ADAMTS5 were clearly expressed in the subchondral bone in MS, MS + Ai, MS + ORX and MS + ORX + Ai group. (d) Semi-quantitative analysis of MMP13 and ADAMTS5 expression comparing the control, MS, MS + Ai, MS + ORX, and MS + ORX + Ai groups. \* $P < 0.033$ , \*\* $P < 0.002$ , \*\*\* $P < 0.001$ , ns = no significance.

expression, a significant increase was observed in the mechanical stress groups compared to the control group. Comparison between the MS and MS + Ai groups revealed that aromatase inhibitor treatment significantly enhanced the expression of both enzymes. Notably, in the MS + Ai + ORX group, the expression levels were markedly elevated (Fig. 4d).

### Effects of 17β-estradiol supplementation on TMJ-OA

In this experiment, comparative analyses were conducted among the 17β-estradiol supplementation group (E2+ group) and the non-supplemented group (E2- group), both following MS + ORX + Ai, as well as the control group.

Paraffin sections of the mandibular condyles from mice were stained with H&E to evaluate cartilage thickness. The 17β-estradiol supplementation (E2+) group showed a significant increase in cartilage thickness compared to the without 17β-estradiol supplementation (E2-) group. However, cartilage thickness and the area of Safranin O-positive staining remained lower than those observed in the control group. Although the modified Mankin score was significantly decreased in the E2+ group compared to the E2- group, it did not return to the level observed in the control group. However, the thickness remained lower than that observed in the control group. In the evaluation of osteoclast numbers by TRAP staining, the E2- group showed a significant increase in osteoclast numbers compared to the control group. However, no significant difference was observed between the E2+ and E2- groups (Fig. 5a, b). Additionally, the expression of MMP13 and ADAMTS5, enzymes involved in cartilage destruction, was weaker in the E2+ group than in the E2- group, while no significant difference was observed between the E2+ and Control groups. Furthermore, the expression of MMP13 and ADAMTS5, which are involved in tissue degradation, was attenuated in the E2+ group compared to the E2- group. However, in comparison to the control group, their expression was still observed around the blood vessels in the subchondral bone (Fig. 5c). In the semi-quantitative analysis, the E2+ group showed a significant reduction in MMP13 and ADAMTS5 expression compared to the E2- group; however, the levels did not return to those observed in the control group (Fig. 5d). PCR analysis of TMJ-OA markers showed significant increases in mRNA expression of *NFκB*, *Gremlin 1*, and *Rela* in the MS group compared to the control group. These increases were more



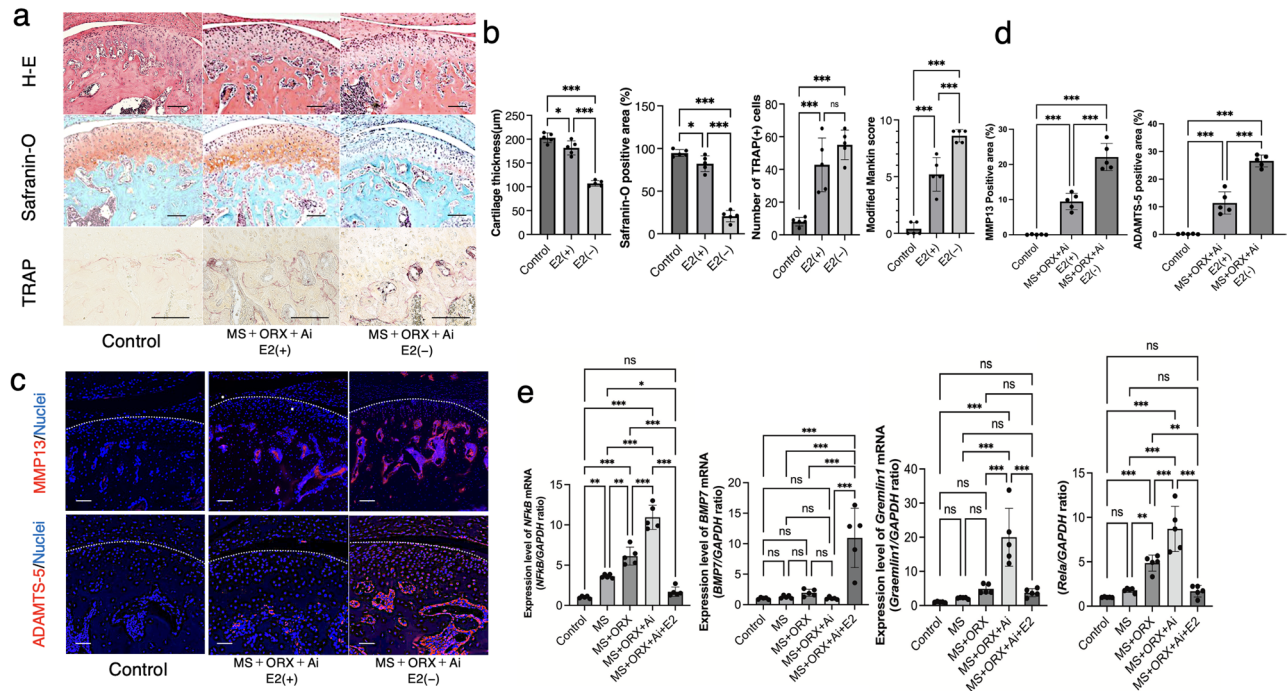


**Fig. 5.** Protective role of 17 $\beta$ -estradiol supplementation in TMJ-OA. Histochemical staining of the mandibular head of male mice is shown as control, E2- (MS + ORX + Ai) and E2+ (MS + ORX + Ai + E2). Cartilage thickness was confirmed by H-E staining (scale bar = 100  $\mu$ m). Positive areas were measured by safranin-O staining (scale bar = 100  $\mu$ m). The number of osteoclasts per mm<sup>2</sup> was measured by TRAP staining (scale bar = 100  $\mu$ m). (b) Cartilage thickness measured in H-E stained sections, proteoglycan area in Safranin-O stained sections was thicker with E2 + than E2-; average number of osteoclasts per mm<sup>2</sup> ( $N > 3$  nuclei) in TRAP stained sections was reduced with E2 +. Modified for OA severity assessment Mankin score for assessing OA severity was greater with E2+. \*\* $P < 0.002$ , \*\*\* $P < 0.001$ , ns = no significance. (c) Immunohistochemical staining of MMP13 (scale bar = 100  $\mu$ m; MMP13: red, nuclei: blue) and ADAMTS5 (scale bar = 100  $\mu$ m; ADAMTS5: red, nuclei: blue) in the mouse mandible head showed that expression was suppressed by E2+. (d) Semi-quantitative analysis of MMP13 and ADAMTS5 expression comparing the control, E2 + and E2 - groups. \* $P < 0.033$ , \*\* $P < 0.002$ , \*\*\* $P < 0.001$ , ns = no significance. (e) Quantitative evaluation of *NFκB*, *BMP7*, *Gremlin1*, and *Rela*, mRNAs involved in TMJ-OA deterioration, by RT-qPCR. Bars indicate each mRNA level relative to *GAPDH* mRNA level ( $n = 5$ ) Data are shown as mean  $\pm$  SD. \* $P < 0.033$ , \*\* $P < 0.002$ , \*\*\* $P < 0.001$ , ns = no significance.

pronounced in the MS + ORX group and reached their highest levels in the MS + ORX + Ai group. In contrast, *BMP7* mRNA expression did not show significant differences among the control, MS, MS + ORX, and MS + ORX + Ai groups. Notably, in the MS + ORX + Ai + E2 group, the mRNA levels of *NFκB*, *Gremlin 1*, and *Rela* were comparable to the control group. Furthermore, *BMP7* mRNA expression in the MS + ORX + Ai + E2 group was significantly upregulated compared to all other groups (Fig. 5e).

## Discussion

The core of this study lies in elucidating the sex-based differences in the pathogenesis of TMJ-OA (temporomandibular joint osteoarthritis). Previous studies have shown that decreased 17 $\beta$ -estradiol levels due to ovariectomy (OVX) in female mice contribute to the progression of TMJ-OA<sup>5,10</sup>. This study focused on male mice to examine the effects of 17 $\beta$ -estradiol and dihydrotestosterone (DHT) on the etiology of TMJ-OA<sup>5</sup>. Aromatase, an enzyme secreted by adipocytes, converts testosterone and DHT into 17 $\beta$ -estradiol. Aromatase inhibition prevents this conversion<sup>16–18</sup>. In this study, administration of an aromatase inhibitor resulted in thinning of mandibular condylar cartilage and increased expression of MMP13 (matrix metalloproteinase-13) and ADAMTS5 (a disintegrin and metalloproteinase with thrombospondin motifs 5). These findings suggest that reduced 17 $\beta$ -estradiol levels compromise cartilage protection, accelerating TMJ-OA progression. Additionally, DHT reduction due to orchietomy (ORX) promoted cartilage destruction through decreased chondrocyte numbers and increased osteoclast activity in the subchondral bone.

In this study, it was confirmed that under excessive mechanical stress (MS), the group treated with aromatase inhibitors exhibited more severe TMJ-OA compared to the orchietomy (ORX) group. This suggests that a reduction in serum 17 $\beta$ -estradiol levels has a greater impact on cartilage destruction in the temporomandibular joint than a reduction in DHT levels. Furthermore, in the group receiving both aromatase inhibitors and orchietomy (Ai + ORX group), both 17 $\beta$ -estradiol and DHT levels were decreased, resulting in a significant reduction in cartilage thickness and Safranin O-positive areas. In this group, the expression of MMP13 and

ADAMTS5 was strongly elevated, indicating accelerated degradation of type II collagen and aggrecan, and the progression of cartilage destruction was faster than in other groups. Additionally, the increase in osteoclast numbers was pronounced, leading to progressive bone destruction, findings consistent with previous reports involving extensive inhibition of  $17\beta$ -estradiol<sup>5,10,19,20</sup>.

In the present study, particularly in the groups subjected to mechanical stress, MMP13 and ADAMTS5 expression was detected not only in the chondrocyte layer but also in the perivascular regions of the subchondral bone. Although these matrix-degrading enzymes are predominantly considered to be chondrocyte-derived, previous reports have demonstrated their expression in other cell types, including fibroblasts, synoviocytes, macrophages, and vascular smooth muscle cells, especially under inflammatory or remodeling conditions<sup>21,22</sup>. These observations suggest that mechanical stress may stimulate the secretion of MMP13 and ADAMTS5 from perivascular cells in the subchondral bone, thereby exacerbating temporomandibular joint degeneration.

In contrast, the E2 + group, which received  $17\beta$ -estradiol supplementation, showed a significant increase in cartilage thickness and Safranin O-positive areas, along with a reduction in modified Mankin scores, confirming the suppressive effects of  $17\beta$ -estradiol on cartilage destruction. These findings align with previous reports suggesting that  $17\beta$ -estradiol plays a critical role in maintaining cartilage homeostasis and preventing cartilage degradation<sup>10,23</sup>. However, no significant differences in osteoclast numbers were observed, consistent with earlier studies indicating that  $17\beta$ -estradiol primarily acts on early osteoclast precursors rather than mature osteoclasts<sup>23</sup>. DHT also plays a role in regulating chondrocyte numbers via growth hormone and insulin-like growth factor 1 (IGF-1)<sup>24,25</sup>. Reduced DHT levels may contribute to cartilage destruction through decreased chondrocyte numbers and increased osteoclast activity in the subchondral bone. Increased VEGF (vascular endothelial growth factor) expression was observed, which is known to enhance MMP expression while suppressing TIMP (tissue inhibitor of metalloproteinases) expression, disrupting the balance of extracellular matrix remodeling and promoting cartilage destruction<sup>16</sup>. VEGF also induces endothelial cells and osteoclasts, exacerbating subchondral bone destruction<sup>6</sup>. Consistent with these findings, this study observed thinning of cartilage and reduced cell density under MS. This aligns with reports that MS induces endoplasmic reticulum stress in chondrocytes, leading to cell death<sup>16</sup>.

This study demonstrated that  $17\beta$ -estradiol and DHT exert protective effects against TMJ-OA through distinct pathways.  $17\beta$ -estradiol is essential for maintaining cartilage homeostasis and contributes to cartilage repair via estrogen receptors (ER $\alpha$  and ER $\beta$ )<sup>24</sup>. DHT, on the other hand, influences chondrocyte numbers and bone metabolism, playing a crucial role in maintaining subchondral bone integrity. These findings advance our understanding of the sex-based mechanisms underlying TMJ-OA and highlight the potential for hormone-based therapeutic strategies. In this study, TMJ-OA was induced in 10-week-old male mice, and specimens were obtained at 19 weeks of age, which corresponds to early adulthood in the mouse lifespan. According to prior reports, this age range is equivalent to the human age range of approximately 20–30 years. During this developmental stage, sex hormone levels in humans begin to diverge significantly between males and females. Notably, the incidence of temporomandibular joint disorders has been reported to increase in females starting from the second and third decades of life, particularly under conditions such as menstrual irregularities or estrogen deficiency. These clinical trends support the translational relevance of our mouse model for studying sex differences in TMJ-OA pathogenesis<sup>13</sup>. E2 + was shown to prevent these detrimental effects. However, further understanding of how E2 exerts its protective effects on the temporomandibular joint is crucial for future treatments. Excessive mechanical stress has been reported to promote osteoarthritis via the *gremlin* 1-NF- $\kappa$ B pathway<sup>26</sup>. *Gremlin* 1 activates NF- $\kappa$ B signaling, leading to the induction of degradative enzymes such as MMP13 and ADAMTS5<sup>27,28</sup>. *Gremlin* 1 is a well-known secreted BMP antagonist that regulates the development of limbs, lungs, kidneys, and retinas by inhibiting BMP signaling<sup>29–31</sup>. *Gremlin* 1 strongly inhibits BMP 2, BMP 4, and BMP 7 by forming heterodimers with them<sup>32</sup>. BMP 7 is highly expressed in the proliferative zone of cartilage and is implicated in hypertrophic differentiation, which contributes to OA development<sup>33</sup>. In addition to BMP inhibition, *Gremlin* 1 affects cellular functions through BMP-independent mechanisms. For instance, VEGFR2 has been identified as a novel receptor for *Gremlin* 1, and the *Gremlin* 1-VEGFR2 pathway exhibits pro-inflammatory effects via NF- $\kappa$ B activation<sup>34–36</sup>. In OA, *Gremlin* 1's regulation of cartilage degradation involves the *Rac1*-ROS-NF- $\kappa$ B pathway, which enhances transcription factors such as NF- $\kappa$ B, HIF-1 $\alpha$ , c-Jun, and Nrf2<sup>37</sup>. Among these factors, *RelA* has been reported to strongly induce *Gremlin* 1 expression<sup>26</sup>. Studies on E2 in lung and breast cancer suggest that E2 suppresses *Gremlin* 1 expression<sup>38–40</sup>. Based on these findings, this study evaluated mRNA expression levels of NF- $\kappa$ B, BMP 7, *Gremlin*-1, and *RelA* to elucidate the protective effects of E2 on the temporomandibular joint. The results demonstrated that E2 supplementation suppressed *Gremlin* 1, NF- $\kappa$ B, and *RelA* expression while enhancing BMP 7 expression. These findings suggest that E2 protects the temporomandibular joint from excessive mechanical stress by inhibiting the *Gremlin* 1-NF- $\kappa$ B pathway via estrogen ER $\alpha$  signaling.

## Conclusion

The lower incidence of TMJ-OA in males compared to females may be attributed to the continuous conversion of testosterone and DHT into  $17\beta$ -estradiol by adrenal aromatase. This process provides protection to the temporomandibular joint against excessive mechanical stress via the *Gremlin* 1-NF- $\kappa$ B pathway. This mechanism differs from the pathway in females, who are prone to TMJ-OA due to menopause or hormonal deficiencies, and may explain why males are less likely to develop TMJ-OA even at older ages. These findings highlight the importance of  $17\beta$ -estradiol in the treatment and prevention of TMJ-OA regardless of sex.

## Materials and methods

### Mice

A total of 90 male C57BL/6 J mice, aged 10 weeks, were obtained from Sankyo Lab Service (Tokyo, Japan) and used in the study. 10-week-old male mice were divided into six groups ( $n = 15$  for each group:  $n = 5$  for Histology/micro-CT,  $n = 5$  for RT-qPCR and for ELISA,  $n = 5$ ): a control group without mechanical stress (control group), a group treated with aromatase inhibitors (Ai group), a group treated with orchiectomy (ORX group), a group treated with aromatase inhibitors and ORX (Ai + ORX group), and groups treated with 17 $\beta$ -estradiol daily (E2 + group) and saline daily (E2 – group) along with Ai + ORX for the experimental protocol (Fig. 1a). All mouse breeding and animal experiments were carried out at the animal facilities of Tokyo Dental College (Tokyo, Japan) with the approval of the Institutional Animal Care and Use Committee of Tokyo Dental College (approval number: 223102, 233106, 233107, 243105, 243106,). Also, mouse studies were performed following the protocol in ARRIVE 2.0 guidelines. All mice were maintained in each cage in our animal facilities and housed in temperature-controlled room at 23 °C under controlled-light/dark cycle. Hard pellets and water were provided for ad libitum consumption.

Orchiectomy (ORX) was performed on the mice under general anesthesia by intraperitoneal administration of a combination of three anesthetics (medetomidine hydrochloride, 0.75 mg/kg, Nippon Zenyaku Kogyo Co., Ltd., Fukushima, Japan; midazolam, 4.0 mg/kg, Sand Co., Tokyo, Japan; butorphanol tartrate, 5.0 mg/kg, Meiji Seika Pharma Stocks Co., Tokyo, Japan). ORX was intended to lower DHT. Sham operations were performed on all groups without ORX. The ALZET pump\* (Model No.2004, Muromachi Machinery Co., Ltd., Tokyo, Japan) was filled with 200  $\mu$ l of an aromatase inhibitor (Letrozole, Tokyo Kasei Kogyo Co., Ltd., Tokyo, Japan) dissolved in dimethyl sulfoxide and diluted with saline to a final concentration of 12.27 mM. Following intraperitoneal implantation, the inhibitor was continuously administered at a rate of 0.25  $\mu$ l/hour for 28 days (16). Aromatase inhibitors were administered to lower 17 $\beta$ -estradiol. Saline solution was administered to the group not receiving the aromatase inhibitor using the ALZET Pump\*. After a 1-week recovery period following orchiectomy, placement of the ALZET Pump\*, and sham surgery, mice were anesthetized, and a metal plate (item number: 21700BZ00197000, Tomy International Inc., Tokyo, Japan) was bonded to the posterior surface of the maxillary portal teeth using dental composite resin to achieve a base thickness of 2 mm (Fig. 1b). Mechanical stress was applied to the mandibular head by inducing an imbalanced occlusion. This added mechanical stress, one of the risk factors for TMJ-OA. The dental composite resin was bonded to the posterior surface of the maxillary portal teeth with a basal thickness of 2 mm to induce an imbalanced occlusion. The post-anesthesia control group did not wear the appliance.

The E2 + group received daily intraperitoneal administration (i.p.) of 0.03  $\mu$ g of 17 $\beta$ -estradiol (E8875; Sigma-Aldrich Co., Ltd., St. Louis, Missouri, USA) in saline as a solvent, while the E2 – group received saline only (4). Administration of E2 confirmed the effect of E2 in DHT lowering conditions.

The mice were weighed weekly to ensure that the study had no effect on body weight. Four weeks after the start of the study, all mice were sacrificed by intraperitoneal administration of 150 mg/kg sodium pentobarbital sodium into the abdominal cavity after induction of general anesthesia using sevoflurane inhalation.

### Measurement of sex hormones in serum

All mice were fasted and given no water for 3 h before collecting blood to standardize the results. Blood was collected using a 5 mm animal lancet (MEDI point, Mineola, NY) and a BD Microtina blood collection tube (Becton Dickinson, Franklin Lakes, NJ). Blood was centrifuged at 13,000 rpm for 10 min, and the collected serum was stored at –20 °C. 17 $\beta$ -estradiol high-sensitivity ELISA kit (Enzo Biochem, Farmingdale, NY, USA), DHT ELISA kit (BioVendor, Brno, Czech Republic) to evaluate serum E2 and DHT levels in the mice. The assay was performed in each group ( $n = 5$ ).

### Microcomputed tomography (micro-CT) analysis

The right femur was fixed with 4% paraformaldehyde (Wako, Osaka) for 2 days and then placed in 70% ethanol. Micro-CT ( $\mu$ CT-50, Scanco Medical AG, Wangen-Brüttisellen, Switzerland) was used to acquire the femur's three-dimensional (3D) images. Image analysis software (TRI/3D-BON; Ratoc System Engineering, Japan) was used to perform bone structure analysis. Micro-CT images were taken with a slice width of 0.01 mm. Trabecular parameters were analyzed in the secondary trabecular region 200  $\mu$ m away from the proximal end of the femoral proximal growth plate. Bone volume per tissue volume (BV/TV), trabecular thickness (Tb.Th), trabecular number (Tb.N), and trabecular spacing (Tb.Spac) were measured ( $n = 5$ ).

### Histomorphometry and immunofluorescence analysis

The mandibular head was sectioned and fixed with 4% paraformaldehyde for 2 days after removing soft tissues. Specimens were decalcified with 10% EDTA solution (Muto Pure Chemicals, Tokyo, Japan) at 4 °C for 4 weeks and embedded in paraffin. The right TMJ was sectioned vertically (5  $\mu$ m thick).

Cartilage thickness was analyzed from H&E-stained sections. The average thickness of cartilage at the mid-coronal portion of the MCC was measured. Averages were calculated for each group ( $n = 5$ ).

TRAP staining was performed using a TRAP staining kit (Sigma-Aldrich, St. Louis, MO, USA) to evaluate osteoclast differentiation in the subchondral bone. The total number of osteoclasts per square millimeter ( $\text{mm}^2$ ) was counted ( $n = 5$ ). TRAP-positive cells with more than three nuclei were counted as osteoclasts.

Safranin O-stained sections were used to examine changes in cartilage breakdown, amounts of proteoglycan, and numbers of chondrocytes in the MCC. Safranin O-positive areas in MCC were determined using ImageJ (National Institutes of Health, Bethesda, MD). The Safranin O-positive area ( $\text{mm}^2$ ) at the mid-coronal portion of the mandibular condylar head was measured, and averages were calculated for each group ( $n = 5$ ).

Modified Mankin scores were evaluated as previously described ( $n = 5$ ).



For immunofluorescence staining, tissue sections were deparaffinized and then placed in 95 °C water containing an Immunosaver Antigen Retriever (Electron Microscopic Stains, Hatfield, PA) for 45 min for antigen activation.

All sections were blocked with PBS supplemented with 1% bovine serum albumin (BSA, Sigma-Aldrich) to reduce nonspecific binding of antigens to the primary antibody. Sections were incubated with the primary antibody (diluted in PBS supplemented with 1% BSA) according to procedures recommended by the manufacturer, as follows: ADAMTS5 rabbit polyclonal antibody as primary antibody (ab182795, Abcam, Cambridge, MA, USA) and MMP13 rabbit polyclonal antibody (LS-C352547, Proteintech, Chicago, IL, USA) as primary antibodies for immunohistochemical staining.

After incubating with primary antibody overnight at 4 °C, the sections were washed three times with PBS. Alexa Fluor 546 Donkey Anti-Rabbit IgG (A10040; Invitrogen, Carlsbad, CA) diluted 1:200 in PBS supplemented with 1% BSA was used for secondary antibody staining. Next, sections were incubated for 2 h with Hoechst 33,342 (Thermo Fisher Scientific, Waltham, MA, USA) to stain cell nuclei. After staining, sections were washed three times with PBS and mounted. Images were acquired using a confocal laser microscope (LSM 880 with Airyscan, Zeiss, Oberkochen, Germany). The percentage of ADAMTS-5 and MMP13-positive areas was measured per standardized image area using immunofluorescence staining.

The groups were separated blindly and two researchers evaluated all scores.

### Reverse transcription quantitative real-time PCR (RT-qPCR) analysis

Total RNA was isolated with TriZol (Invitrogen), and the isolated mRNA was evaluated in quantity and quality using a Nanodrop ND-100 spectrophotometer (Thermo Scientific, Waltham, MA). mRNA was converted to cDNA using ReverTra Ace qPCR RT Master Mix with gDNA Remover (Toyobo, Osaka, Japan). For RT-qPCR, a reaction mixture was prepared with Thunderbird SYBR qPCR Mix (Toyobo), paired primers, and a defined amount of template cDNA. RT-qPCR reactions were carried out using the following primer sets for *GAPDH*, *NFκB*, *BMP7*, *Gremlin1* and *Rela*: *GAPDH*: 5'- GTCTCCTCTGACTTCAACAGCG-3' and 5'- ACCACCCTGTTGCTGTAGCCAA-3'; *NFκB*: 5'- TGATCCATATTTGGGAAGGCCTGA-3' and 5'- GTATGGGCCATCTGTTGGCAG-3'; *BMP7*: 5'- TCCAAGACGCCAAAGAACCAAGAG-3' and 5'- CCTTCAGGTGCAATGATCCAGTCC-3'; *Gremlin1*: 5'- TATGAGCCGCACAGCCTA CA-3' and 5'- GCACCTTGGGACCCTTTCTT-3'; *Rela*: 5'- TGAACCAGGGCATACCTGTG-3' and 5'- CCCCTGTCACTAGGC GAGTT-3'. RT-qPCR was performed using a QuantStudio 7pro system (Applied Biosystems, Foster City, CA). Initial denaturation was induced at 95 °C for 24 s, followed by 40 cycles of denaturation at 95 °C for 3 s, annealing at 60 °C for 5 s, and elongation at 72 °C for 45 s. The relative expression ratio of markers was calculated based on the ddCt comparative threshold cycle (CT) method. The calculated values were normalized against an internal control (*GAPDH*). Five technical replicates were analyzed for RT-qPCR.

### Statistical analysis

All data were statistically analyzed using GraphPad Prism 9 (MDF, Tokyo, JAPAN). Between-group comparisons were performed with Tukey test. Comparisons with the control group was performed using Dunnett's test. Significant differences were indicated in accordance with APA style; a P value of 0.033 or less was considered a significant difference. The One-way ANOVA models were tested on the assumptions of "normality" and "homoscedasticity." The sample size was calculated with the statistical power of 80%, significance level of 5%, and effect size of 1.8.

### Data availability

All data generated or analyzed during this study are included in this published article. Furthermore, the data availability statement has been provided in the submission system, as per the journal's guidelines.

Received: 15 February 2025; Accepted: 20 May 2025

Published online: 28 May 2025

### References

- Cardoneanu, A., Macovei, L. A., Burlui, A. M., Mihai, I. R. & Bratoiu, I. Temporomandibular joint osteoarthritis: pathogenic mechanisms involving the cartilage and subchondral bone, and potential therapeutic strategies for joint regeneration. *Int. J. Mol. Sci.* **24**, 171 (2022).
- Wang, X. D., Zhang, J. N., Gan, Y. H. & Zhou, Y. H. Current Understanding of pathogenesis and treatment of TMJ osteoarthritis. *J. Dent. Res.* **94**, 666–673 (2015).
- Robinson, J. L., Iwasaki, L. R., Schneider, D. A., Nickel, J. C. & Allen, K. D. Sex differences in the estrogen-dependent regulation of temporomandibular joint remodeling in altered loading. *Osteoarthr. Cartil.* **25**, 533–543 (2017).
- Chang, C. L., Wang, D. H., Yang, M. C., Hsu, W. E. & Hsu, M. L. Functional disorders of the temporomandibular joints: internal derangement of the temporomandibular joint. *Kaohsiung J. Med. Sci.* **34**, 223–230 (2018).
- Ootake, T. et al. Effects of mechanical stress and deficiency of dihydrotestosterone or 17β-estradiol on temporomandibular joint osteoarthritis in mice. *Osteoarthr. Cartil.* **29**, 1575–1589 (2021).
- Mino-Oka, A. et al. Roles of hypoxia inducible factor-1α in the temporomandibular joint. *Arch. Oral Biol.* **73**, 274–281 (2017).
- Bianchi, J., Pinto, A. D. S., Ignácio, J., Ryan, O., Gonçalves, J. R. & D. P. & Effect of temporomandibular joint articular dislocation on anterior open-bite malocclusion: an orthodontic-surgical approach. *Am. J. Orthod. Dentofac. Orthop.* **152**, 848–858 (2017).
- Sperry, M. M., Yu, Y. H., Kartha, S., Ghimire, P. & Welch, R. L. Intra-articular etanercept attenuates pain and hypoxia from TMJ loading in the rat. *J. Orthop. Res.* **38**, 1316–1326 (2020).
- Atasoy-Zeybek, A., Showel, K. K., Nagelli, C. V., Westendorf, J. J. & Evans, C. H. The intersection of aging and Estrogen in osteoarthritis. *NPJ Womens Health.* **3**, 15 (2025).
- Wu, Y., Kadota-Watanabe, C., Ogawa, T. & Moriyama, K. Combination of Estrogen deficiency and excessive mechanical stress aggravates temporomandibular joint osteoarthritis in vivo. *Arch. Oral Biol.* **102**, 39–46 (2019).

11. Dreier, R., Ising, T., Ramroth, M. & Rellmann, Y. Estradiol inhibits ER Stress-Induced apoptosis in chondrocytes and contributes to a reduced Osteoarthritic cartilage degeneration in female mice. *Front. Cell. Dev. Biol.* **10**, 913118 (2022).
12. Lu, Z., Zhang, A., Wang, J., Han, K. & Gao, H. Estrogen alleviates post-traumatic osteoarthritis progression and decreases p-EGFR levels in female mouse cartilage. *BMC Musculoskelet. Disord.* **23**, 685 (2022).
13. Patel, J., Chen, S., Katzmeyer, T., Pei, Y. A. & Pei, M. Sex-dependent variation in cartilage adaptation: from degeneration to regeneration. *Biol. Sex. Differ.* **14**, 17 (2023).
14. Ha-neui, K., Filipa, P., Intawat, N., Ferreira, S. & Ramos, P. Estrogens decrease osteoclast number by attenuating mitochondria oxidative phosphorylation and ATP production in early osteoclast precursors. *Sci. Rep.* **10** <https://doi.org/10.1038/s41598-020-68890-7> (2020).
15. Okubo, Y., Sekiguchi, K., Saito, T., Nakamura, K. & Mori, K. Visualization of  $Ca^{2+}$  filling mechanisms upon synaptic inputs in the Endoplasmic reticulum of cerebellar purkinje cells. *J. Neurosci.* **35**, 15837–15846 (2015).
16. Krishnan, A., Bala, S., Venkatesh, J., Ramachandran, R. & Pillai, S. M. Effect of DHT-induced hyperandrogenism on the pro-inflammatory cytokines in a rat model of polycystic ovary morphology. *Med. (Kaunas)*. **56**, 100 (2020).
17. Vari, C. E., Ósz, B. E., Miklos, A., Berbecaru-Iovan, A. & Tero-Vescan, A. Aromatase inhibitors in men – off-label use, misuse, abuse and doping. *FARMACIA* **64**, 813–818 (2016).
18. Rambhatla, A., Mills, J. N. & Rajfer, J. The role of Estrogen modulators in male hypogonadism and infertility. *Rev. Urol.* **18**, 66–72 (2016).
19. Komrakova, M. et al. A combined treatment with selective androgen and Estrogen receptor modulators prevents bone loss in orchietomized rats. *J. Endocrinol. Invest.* **45**, 2299–2311 (2022).
20. Ha-Neui et al. Estrogens decrease osteoclast number by attenuating mitochondria oxidative phosphorylation and ATP production in early osteoclast precursors. *Sci. Rep.* **10**, 11933 (2020).
21. Ponte, F. et al. Mmp13 deletion in mesenchymal cells increases bone mass and May attenuate the cortical bone loss caused by Estrogen deficiency. *Sci. Rep.* **12**, 10257 (2022).
22. Kirman, D. C. et al. Cell surface nucleolin is a novel ADAMTS5 receptor mediating endothelial cell apoptosis. *Cell. Death Dis.* **13**, 172 (2022).
23. Lara-Castillo, N. Estrogen signaling in bone. *Appl. Sci.* **11**, 4439 (2021).
24. Dixit, M., Poudel, S. B. & Yakar, S. Effects of GH/IGF axis on bone and cartilage. *Mol. Cell. Endocrinol.* **519**, 111052 (2021).
25. Xiao, M., Hu, Z. H., Jiang, H. H., Fang, W. & Long, X. Role of osteoclast differentiation in the occurrence of osteoarthritis of temporomandibular joint. *Eur. J. Oral Sci.* **39**, 398–404 (2021).
26. Chang, S. H. et al. Excessive mechanical loading promotes osteoarthritis through the gremlin-1-NF- $\kappa$ B pathway. *Nat. Commun.* **10**, 1442. <https://doi.org/10.1038/s41467-019-09491-5> (2019).
27. Jiang, L. et al. ADAMTS5 in osteoarthritis: biological functions, regulatory network, and potential targeting therapies. *Front. Mol. Biosci.* **8**, 703110 (2021).
28. Huang, X. et al. Dickkopf-related protein 1 and Gremlin 1 show different response than frizzled-related protein in human synovial fluid following knee injury and in patients with osteoarthritis. *Osteoarthr. Cartil.* **26**, 834–843 (2018).
29. Brazil, D. P., Church, R. H., Surrae, S., Godson, C. & Martin, F. BMP signalling: agony and antagonism in the family. *Trends Cell. Biol.* **25**, 249–264 (2015).
30. Church, R. H. et al. Gremlin1 plays a key role in kidney development and renal fibrosis. *Am. J. Physiol. Ren. Physiol.* **312**, F1141–F1157 (2017).
31. Wang, Y. H., Keenan, S. R., Lynn, J., McEwan, J. C. & Beck, C. W. Gremlin1 induces anterior-posterior limb bifurcations in developing *Xenopus* limbs but does not enhance limb regeneration. *Mech Dev* **138 Pt. 3**, 256–267 (2015).
32. Elemam, N. M., Malek, A. I., Mahmoud, E. E., El-Huneidi, W. & Talaat, I. M. Insights into the role of Gremlin-1, a bone morphogenic protein antagonist, in Cancer initiation and progression. *Biomedicines* **10**, 301 (2022).
33. Jaswal, A. P. et al. BMP signaling: A significant player and therapeutic target for osteoarthritis. *Osteoarthr. Cartil.* **31**, 1454–1468 (2023).
34. Chang, S. H. et al. Excessive mechanical loading promotes osteoarthritis through the gremlin-1-NF- $\kappa$ B pathway. *Nat. Commun.* **10**, 1442 (2019).
35. Corsini, M. et al. Cyclic adenosine monophosphate-response element-binding protein mediates the proangiogenic or Proinflammatory activity of Gremlin. *Arterioscler. Thromb. Vasc Biol.* **34**, 136–145 (2014).
36. Lavoie, C. et al. Gremlin regulates renal inflammation via the vascular endothelial growth factor receptor 2 pathway. *J. Pathol.* **236**, 407–420 (2015).
37. Gao, X. & Schöttker, B. Reduction-oxidation pathways involved in cancer development: a systematic review of literature reviews. *Oncotarget* **8**, 51888–51906. <https://doi.org/10.18632/oncotarget.17128> (2017).
38. Park, S. A. et al. Gremlin-1 augments the oestrogen-related receptor alpha signalling through EGFR activation: implications for the progression of breast cancer. *Br. J. Cancer.* **123**, 988–999 (2020).
39. Neckmann, U. et al. GREM1 is associated with metastasis and predicts poor prognosis in ER-negative breast cancer patients. *Cell. Commun. Signal.* **17** <https://doi.org/10.1186/s12964-019-0467-7> (2019).
40. Frump, A. L. et al. Estrogen receptor-dependent Attenuation of hypoxia-induced changes in the lung genome of pulmonary hypertension rats. *Pulm Circ.* **7**, 232–243 (2017).

## Acknowledgements

The authors thank Satoru Matsunaga (Department of Oral Anatomy, Tokyo Dental College, Tokyo, Japan), Takashi Nakamura (Department of Biochemistry, Tokyo Dental College, Tokyo, Japan) and Toshihide Mizoguchi (Oral Science Research Center, Tokyo Dental College, Tokyo, Japan), for technical assistance with the histomorphometry analysis and genetic analysis.

## Author contributions

Conceptualization, T.T., T.I. and Y.N.; methodology, T.T., T.I., N.K. and Y.N.; data curation, T.T., T.I., N.K. and Y.N.; writing—original draft preparation, T.T. and T.I.; writing—review and editing, T.T., T.I., N.K. and Y.N.; visualization, T.T., T.I., N.K. and Y.N.; supervision, T. I. and Y.N.; project administration, T.T., T.I., K.N. and Y.N. All authors have read and agreed to the published version of the manuscript.

## Funding

This work was supported by JSPS KAKENHI Grant Number JP20 K10215. In addition, research grant was received from Tokyo Dental College.

## Declarations

### Competing interests

The authors declare no competing interests.

### Ethical approval

The experimental protocol of this study was approved by the Animal Welfare Committee of Tokyo Dental College based on the Animal Care Standards of this institution (approval no. 223102, 233106, 233107, 243105, 243106). All experiments were conducted in accordance with relevant institutional and international guidelines and regulations, including the ARRIVE 2.0 guidelines and the Guide for the Care and Use of Laboratory Animals published by the National Institutes of Health (NIH). This study does not involve human participants, and therefore, informed consent was not required.

### Additional information

**Correspondence** and requests for materials should be addressed to T.I.

**Reprints and permissions information** is available at [www.nature.com/reprints](http://www.nature.com/reprints).

**Publisher's note** Springer Nature remains neutral with regard to jurisdictional claims in published maps and institutional affiliations.

**Open Access** This article is licensed under a Creative Commons Attribution-NonCommercial-NoDerivatives 4.0 International License, which permits any non-commercial use, sharing, distribution and reproduction in any medium or format, as long as you give appropriate credit to the original author(s) and the source, provide a link to the Creative Commons licence, and indicate if you modified the licensed material. You do not have permission under this licence to share adapted material derived from this article or parts of it. The images or other third party material in this article are included in the article's Creative Commons licence, unless indicated otherwise in a credit line to the material. If material is not included in the article's Creative Commons licence and your intended use is not permitted by statutory regulation or exceeds the permitted use, you will need to obtain permission directly from the copyright holder. To view a copy of this licence, visit <http://creativecommons.org/licenses/by-nc-nd/4.0/>.

© The Author(s) 2025